Osteoarthritis and Cartilage 23 (2015) 1483–1490

Osteoarthritis and Cartilage

OARSI OSTEOARTHRITIS RESEARCH SOCIETY INTERNATIONAL

Knee osteoarthritis patients with severe nocturnal pain have altered proximal tibial subchondral bone mineral density

W.D. Burnett †, S.A. Kontulainen † ‡, C.E. McLennan §, D. Hazel §, C. Talmo §, D.J. Hunter ‖, D.R. Wilson ¶, J.D. Johnston † # *

† *Division of Biomedical Engineering, University of Saskatchewan, Saskatoon, SK, Canada*
‡ *College of Kinesiology, University of Saskatchewan, Saskatoon, SK, Canada*
§ *Division of Research, New England Baptist Hospital, Boston, MA, USA*
‖ *Institute of Bone and Joint Research, University of Sydney, Sydney, NSW, Australia*
¶ *Department of Orthopaedics and Centre for Hip Health and Mobility, University of British Columbia and Vancouver Costal Health Research Institute, Vancouver, BC, Canada*
# *Department of Mechanical Engineering, University of Saskatchewan, SK, Canada*

ARTICLE INFO

Article history:
Received 2 October 2014
Accepted 14 April 2015

Keywords:
Osteoarthritis
Knee
Pain
Subchondral bone
Proximal tibia
Computed tomography

SUMMARY

Objective: Our objective was to investigate relationships between proximal tibial subchondral bone mineral density (BMD) and nocturnal pain in patients with knee osteoarthritis (OA).
Methods: The preoperative knee of 42 patients booked for knee arthroplasty was scanned using quantitative computed tomography (QCT). Pain was measured using the Western Ontario and McMaster Universities Arthritis Index (WOMAC) and participants were categorized into three groups: 'no pain', 'moderate pain', and 'severe pain' while lying down at night. We used depth-specific image processing to assess tibial subchondral BMD at normalized depths of 0–2.5 mm, 2.5–5.0 mm and 5–10 mm relative to the subchondral surface. Regional analyses of each medial and lateral plateau included total BMD and maximum BMD within a 10 mm diameter core or 'focal spot'. The association between WOMAC pain scores and BMD measurements was assessed using Spearman's rank correlation. Regional BMD was compared pairwise between pain and no pain groups using multivariate analysis of covariance using age, sex, and BMI as covariates and Bonferroni adjustment for multiple comparisons.
Results: Lateral focal BMD at the 2.5–5 mm depth was related to nocturnal pain ($\rho = 0.388$, $P = 0.011$). The lateral focal BMD was 33% higher in participants with 'severe pain' than participants with 'no pain' at 2.5–5 mm depth ($P = 0.028$) and 32% higher at 5–10 mm depth ($P = 0.049$). There were no BMD differences at 0–2.5 mm from the subchondral surface.
Conclusion: This study suggests that local subchondral bone density may have a role in elucidating OA-related pain pathogenesis.

Introduction

Knee osteoarthritis (OA) is a leading cause of chronic pain and disability in the elderly[1]. Pain is the dominant symptom of OA[2] and is often the first indication that patients may be afflicted with OA. OA-related pain is complex[3,4], as it is a combination of social, psychological, and biological factors, with no simple unitary concept linking symptoms with structural damage[5]. Within the joint structure, pain could be due to the presence of various contributing factors (e.g., altered joint alignment, joint instability, osteophyte presence both peripherally and within the joint, inflammation, cyst presence, altered subchondral bone properties, bone marrow lesions (BMLs)). Importantly, underlying sources of pain may be masked by specific structural factors, such as altered joint alignment, osteophyte presence, and inflammation, which would likely present during dynamic weight-bearing activities such as climbing stairs or walking. To isolate potential underlying sources of pain, it is advantageous to study pain with non-weight bearing activities, such as lying in bed at night. Understanding

* Address correspondence and reprint requests to: J.D. Johnston, Department of Mechanical Engineering, University of Saskatchewan, 57 Campus Dr., Saskatoon, SK S7N 1G9, Canada. Tel: 1-306-966-1468.
E-mail address: james.johnston@usask.ca (J.D. Johnston).

http://dx.doi.org/10.1016/j.joca.2015.04.012

potential sources of pain during non-weight bearing activities, such as nocturnal pain, is also relevant as it is related to sleeplessness and other disruptions to quality of life in OA patients[6].

Knee OA is commonly characterized by subchondral bone changes, including altered subchondral bone thickness[7], bone volume fraction[8] and volumetric density[9,10], as well as the presence of BMLs as observed *via* magnetic resonance imaging (MRI)[11–13]. Little is known regarding associations between pain and altered subchondral bone morphology or density; however, BML presence and size have both shown strong associations with knee pain[4,13–17]. Of relevance to this study, BMLs have been shown to be associated with increased bone mineral density (BMD)[12] and have higher local BMD than surrounding bone tissue[11]. Importantly, altered BMD may disrupt local innervation[18] and/or the local mechanical behaviour of bone[19], and thus may be a factor in OA-related knee pain.

Our current understanding of the relationship between pain and altered BMD primarily relies on evidence from studies using two-dimensional (2D) dual-energy absorptiometry (DXA)[20,21]. However, these studies provide conflicting results, reporting that both higher areal BMD (aBMD)[20] and lower aBMD[21] are associated with OA-related pain. These conflicting results may be due to the inherent limitations of 2D projection techniques, such as patient size and positioning[22], unstandardized regions of interest (ROI)[12,21,23], and the inability to evaluate distinct regions or depths[22]. Three-dimensional (3D) computed tomography (CT) based depth-specific imaging techniques have the ability distinguish differences in subchondral volumetric BMD between normal and OA tibiae[10,24], and may have the ability to identify regional BMD differences in patients with and without pain. Depth-specific imaging techniques also have the potential to determine approximate contrasts between subchondral cortical BMD and less dense trabecular BMD layers[25], which may have different roles in OA-related pain.

Using a depth-specific CT-based image processing tool, the objective of this study was to determine whether there are associations between proximal tibial subchondral BMD and OA-related nocturnal pain.

Methods

Study participants

Fifty-two participants (23M: 29F; mean age 64, SD ± 9.4years) with OA were recruited prior to total knee replacement. Study exclusion criteria included: pregnant women, patients having a revision replacement instead of primary knee replacement, and patients with a prior history of bone pathology at the knee joint. CT images with excessive imaging artifacts, motion artifacts, or incomplete images were excluded, resulting in 42 study participants (17M: 25F; 64 ± 10 years). The Institutional Research Board of the New England Baptist Hospital approved the study. Informed consent was obtained from all study participants.

Knee assesment

OA severity was classified using Kellgren–Lawrence grading[26] and OA-related pain severity was measured at the affected knee joint using a 5-point Likert scale (0–4) of the pain subsection of the Western Ontario McMasters Osteoarthritis Index (WOMAC)[27]. Participants were asked to assess the level of pain in the affected knee joint within the past 24-h while walking on a flat surface, going up or down stairs, nocturnal pain at night in bed, sitting or lying down, and standing upright. This study was focused on non-weight bearing nocturnal pain at night in bed.

To help explain potentially high and low BMD findings, all CT scans (including axial, sagittal, and coronal reconstructions) were retrospectively evaluated for cyst presence, altered knee alignment, and joint laxity. Cyst size and number was semi-qualitatively scored using a simple combined scoring system (none, small, moderate, large) similar to the atlas system of Altman and Gold[28] (none, mild, moderate, severe). Knee alignment was characterized as varus, valgus, and neutral. Joint laxity was identified based upon evidence of medial or lateral shifting of the femur relative to the tibia. A single researcher (JDJ), trained by an experienced orthopaedic surgeon who routinely assessed cyst presence and knee alignment/laxity, performed all scorings.

CT acquisition

We used a single energy clinical CT scanner (LightSpeed 4-slice, General Electric, Milwaukee, WI, USA) for bone imaging. A solid quantitative CT (QCT) reference phantom of known bone mineral densities (Model 3T, Mindways Software Inc., Austin, TX, USA) was placed under the participants and included in all CT scans. The phantom was included to convert grayscale CT Hounsfield Units (HU) to equivalent apparent BMD (mg/cm^3 K_2HPO_4) with both human and animal studies verifying that QCT density measures are accurate representations of true BMD[29,30]. Participants were oriented supine within the CT gantry and both legs were simultaneously scanned. Scans included the distal femur, patella, proximal tibia, and the 66% tibial shaft site proximal to the distal tibial endplate[31]. Only the proximal tibia and the 66% tibial shaft site were used in the current analysis.

CT scanning parameters included: 120 kVp tube voltage, 150 mAs tube current-time product, axial scanning plane, 0.625 mm isotropic voxel size (0.625 slice thickness, 0.625 mm × 0.625 mm in-plane pixel size), ~250 slices, ~60 sec scan time. A standard bone kernel (BONE) was used for CT image post-processing. Effective radiation dose was ~0.073 mSv per scan, estimated using shareware software (CT-DOSE, National Board of Health, Herley, Denmark). For comparison, the average effective radiation dose during a trans-atlantic flight from Europe to North America is about 0.05 mSv[32].

CT image analysis

We used an earlier developed depth-specific image processing technique (computed tomography topographical mapping of subchondral density, CT-TOMASD)[24,33] to measure subchondral proximal tibial subchondral BMD. A single user (WDB) performed all image processing and segmentations. A precision study was performed on an independent sample using recommended techniques[34] and results were compared to previously published results from another user[33]. Precision errors (root mean square coefficients of variation, CV%)[34] ranged from 0.7% to 3.6%, and absolute percent differences in regional mean BMD between both users were all below 3%.

This method uses surface projection image processing to quantify volumetric subchondral bone density at user-defined depths from the subchondral bone surface. Briefly, equivalent volumetric BMD (mg/cm^3 K_2HPO_4) values were converted from grayscale HU using subject-specific linear regression equations developed from known densities within the QCT phantom included in each individual axial image ($r^2 > 0.99$) (Matlab 2010b; MathWorks, Natick, MA, USA)[24]. Subject-specific half maximum height thresholds[35] were then determined to define the proximal tibial subchondral surface. Serial images were individually segmented using semi-automatic region growing and manual correction techniques using commercial software (Analyze10.0; Mayo Foundation, Rochester, MN, USA) and an interactive touch-screen tablet

(Cintiq 21UX; Wacom, Krefeld, Germany), then grouped to build a 3D image volume. Medial and lateral plateau surfaces were then defined by manually selecting boundary points. Each plateau was then realigned and reconstructed relative to "best-fit" planes passing through the defined boundary points (Matlab 2010b) for surface projection analyses. Previously defined boundary points were then manually adjusted (using knot points and natural cubic splines), to ensure that the analysis region did not overlay high-density cortical edges, the tibial spine, or osteophytes[24,33].

To allow for subject-to-subject comparisons, subject-specific depth was normalized based on user-defined depth, relative proximal tibia volume (volume superior to lateral inferior ridge of the proximal fibular head), and area (both lateral and medial plateaus) by using the following equation:

$$\frac{d_{ss} \times area_{ss}}{d \times area_m} = \frac{volume_{ss}}{volume_m}$$

where $volume_{ss}/volume_m$ is a relative volume ratio defined by dividing each subject-specific proximal tibia volume by the mean proximal tibia volume of all specimens, $area_{ss}$ is the subject-specific (segmented) area of the medial and lateral plateaus, $area_m$ is mean area of all subjects, d is the desired user-defined normalized depth (i.e., 2.5 mm), and d_{ss} is the actual subject-specific depth corresponding to the user-defined normalized depth[24].

We evaluated total lateral and total medial plateau BMD, as well as average maximum BMD of a 10 mm diameter core or 'focal spot' which searched each lateral and medial plateau for a maximum value[33] (Fig. 1). We included focal analyses to locate small regions of high-density bone possibly masked by whole compartment analyses. All analyses were performed at three normalized depths from the subchondral surface:

(1) 0–2.5 mm, approximating the density of subchondral endplate and cortical bone[36], (2) 2.5–5 mm, approximating the density of subchondral trabecular bone, and (3) 5–10 mm, approximating the density of proximal epiphyseal trabecular bone[10].

Statistical analysis

To examine associations between nocturnal pain at night in bed and proximal tibial subchondral BMD, we used Spearman's rank correlation. We report Spearman's rank correlation coefficients (ρ) for all associations.

We categorized participants into three groups based on their WOMAC score of pain at night in bed. Patients with a score of 0 or 1 were considered to have 'no pain', patients with a score of 2 were considered to have 'moderate pain', and patients with a score of 3 or greater were considered to have 'severe pain'[38]. To compare differences in proximal tibial subchondral BMD across patients with 'no pain' and patients experiencing either 'moderate pain' or 'severe pain' at night in bed, we used multivariate analysis of covariance (MANCOVA) and selected age, sex, and BMI as covariates[37]. We report the *F*-statistic for BMD measures with significant between-group differences. We also performed pair-wise comparisons with Bonferroni adjustment for multiple comparisons to determine individual group differences between pain ('severe pain' and 'moderate pain') and 'no pain' for each BMD measure. We report mean and standard deviation (SD), adjusted mean differences, and 95% confidence intervals. We also used MANCOVA to compare cortical cross-sectional area and density at the tibia shaft across pain groups, also adjusting for age, sex and BMI[37]. Statistical significance was defined as $P < 0.05$, and statistical analyses were performed using SPSS 21.0 (IBM, Armonk, NY, USA).

Results

The characteristics of study participants, including cyst presence and joint alignment/laxity, are shown in Table I. Patients had OA severity of KL grade ranging from 3 to 4. In the WOMAC assessment of non-weight bearing pain at night in bed, scores ranged from 0 (none) to 4 (extreme). Participants were divided into three groups based on pain at night in bed: 'no pain' ($n = 17$), 'moderate pain' ($n = 16$), and 'severe pain' ($n = 9$).

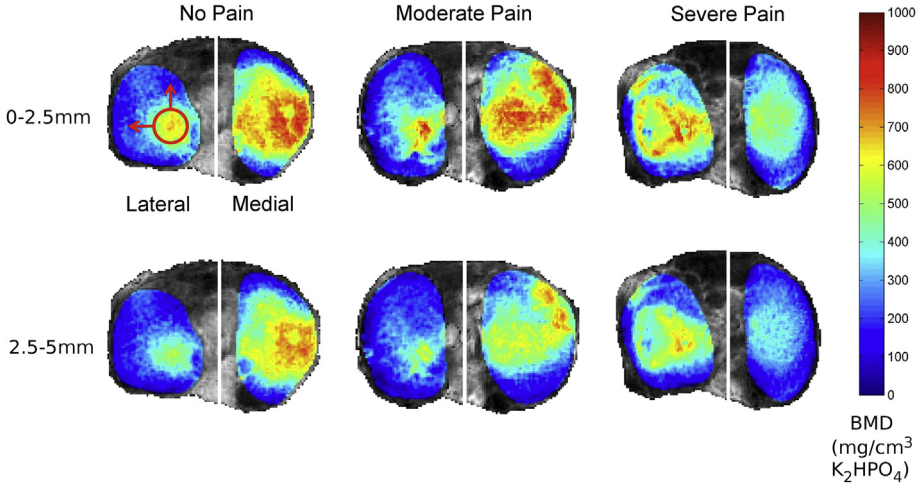

Fig. 1. Representative topographical colormaps of proximal tibial BMD at depths of 0–2.5 mm (top row) and 2.5–5 mm (bottom row) in one participant reporting 'no pain', 'moderate pain', and 'severe pain' at night in bed. Regional analysis includes average BMD of the lateral and medial plateaus, and average maximum BMD of a 10 mm diameter focal spot (shown in upper left-hand image) localized on the maximum value of each lateral and medial plateau.

Internal control

We compared cortical cross-sectional area and density of the tibia shaft (66% of tibia length, proximal from distal tibia plateau)[31] to assess possible between-group differences in local (e.g., mechanical loading) and systemic factors (e.g., nutrition, medication)[37].

Spearman's rank coefficients showed a significant association between pain at night in bed and lateral focal BMD at a depth of 2.5–5 mm from the subchondral surface ($\rho = 0.388$, $P = 0.011$). There were no other significant associations between pain scores and other BMD metrics (Table II).

Table I
Background characteristics and clinical data for study participants and groups

Characteristic	All Participants ($n = 42$)	'No Pain' ($n = 17$)	'Moderate Pain' ($n = 16$)	'Severe Pain' ($n = 9$)
WOMAC (in bed at night)		0 or 1	2	3 or 4
Sex ratio (M:F)	17:25	7:10	7:9	3:6
Age (mean ± SD)	64.1 ± 10.1	67.5 ± 9.1	61.8 ± 11.0	61.8 ± 9.3
BMI (mean ± SD)	28.7 ± 3.7	28.3 ± 4.1	29.1 ± 3.6	28.7 ± 3.0
Side (L:R)	18:24	7:10	6:10	5:4
OA Severity (KL)	3 to 4	3 to 4	3 to 4	3 to 4
Cysts (none/small/moderate/large)	31%/24%/26%/19%	47%/35%/12%/6%	31%/13%/25%/31%	0%/22%/56%/22%
Alignment (varus/neutral/valgus)	67%/14%/19%	71%/24%/6%	75%/6%/19%	44%/11%/44%
Laxity (medial/neutral/lateral)	21%/79%/0%	12%/88%/0%	19%/81%/0%	44%/56%/0%

Table II
Spearman rank correlation coefficients (ρ) for relationship between BMD measurements and WOMAC pain score while lying down at night. Bolded values indicate $P < 0.05$

Side	Region	Depth from subchondral surface		
		0–2.5 mm	2.5–5 mm	5–10 mm
Medial	Total	−0.284 ($P = 0.069$)	−0.244 ($P = 0.120$)	−0.218 ($P = 0.165$)
	Focal BMD	−0.211 ($P = 0.181$)	−0.223 ($P = 0.157$)	−0.248 ($P = 0.113$)
Lateral	Total	0.290 ($P = 0.062$)	0.301 ($P = 0.053$)	0.203 ($P = 0.198$)
	Focal BMD	−0.156 ($P = 0.323$)	**0.388 ($P = 0.011$)**	0.290 ($P = 0.063$)

After adjusting for covariates, there was a significant between-group difference in lateral focal BMD at depths of 2.5–5 mm ($F(2,36) = 3.915$, $P < 0.05$) and 5–10 mm ($F(2,36) = 3.258$, $P < 0.05$) from the subchondral surface. Individual group differences showed that participants with 'severe pain' had higher lateral focal BMD than participants with 'no pain' at depths of 2.5–5 mm (33% higher; adjusted mean difference: 114 mg/cm^3; 95% CI: 9.6–218 mg/cm^3; $P = 0.028$) and 5–10 mm (32% higher; adjusted mean difference: 60 mg/cm^3; 95% CI: 0.3–120 mg/cm^3; $P = 0.049$) (Table IV). There were no significant differences in focal BMD between groups at depths of 0–2.5 mm from the subchondral surface, or at the total lateral or medial plateaus (Fig. 2, Tables III and IV). However, there was a statistically non-significant trend for lower BMD at the medial plateau (across all depths) across the groups with increasing pain (Fig. 2, Tables III and IV). At the tibial shaft, there were no significant differences in cortical cross-sectional area ($F(2,36) = 0.208$, $P > 0.05$) or density ($F(2,36) = 0.186$, $P > 0.05$) between groups.

Discussion

Our depth-specific imaging technique identified a positive association between lateral focal BMD at the 2.5–5 mm depth and non-weight bearing pain at night in bed. Isolated comparisons identified higher lateral focal BMD at depths 2.5–5 mm and 5–10 mm from the proximal tibial subchondral surface in patients experiencing 'severe pain' than in patients experiencing 'no pain' at night in bed. This is the first study to assess the relationship between depth-specific proximal tibial subchondral BMD and symptomatic OA. These findings suggest that there may be previously overlooked characteristics in proximal tibial subchondral BMD, such as focal BMD at depths greater than 2.5 mm from the subchondral surface, which may have a role in OA-related pain pathogenesis.

Our findings are consistent with prior research showing associations between pain and subchondral bone, namely BML presence[4,13–17]. Recent research has also shown BMLs to have higher

Table III
Pair-wise comparison of tibial BMD measurements in patients with knee OA with 'no pain' and 'moderate pain' while lying down at night, including mean ± SD, adjusted mean difference, percent difference from 'no pain', 95% confidence interval (CI), and *P*-value

Region	Depth	BMD (mg/cm^3 K_2HPO_4)		Adjusted mean difference* from No Pain (%)	95% confidence interval (mg/cm^3 K_2HPO_4)		*P*-value
		No Pain	Moderate Pain				
		Mean ± SD	Mean ± SD		Lower limit	Upper limit	
Medial plateau							
Total	0–2.5 mm	480 ± 93	437 ± 116	−53 (−10.9%)	−146	41	0.50
	2.5–5 mm	322 ± 98	296 ± 91	−36 (−11.0%)	−122	49	0.90
	5–7.5 mm	203 ± 85	177 ± 61	−35 (−17.0%)	−102	31	0.57
Focal BMD	0–2.5 mm	658 ± 94	631 ± 108	−38 (−5.6%)	−127	51	0.88
	2.5–5 mm	499 ± 130	474 ± 123	−37 (−7.4%)	−152	77	1.00
	5–7.5 mm	347 ± 135	309 ± 94	−49 (−14.0%)	−152	54	0.71
Lateral plateau							
Total	0–2.5 mm	339 ± 62	356 ± 112	19 (5.6%)	−58	96	1.00
	2.5–5 mm	198 ± 52	214 ± 80	17 (8.4%)	−44	77	1.00
	5–7.5 mm	127 ± 38	128 ± 45	0 (0%)	−38	38	1.00
Focal BMD	0–2.5 mm	596 ± 81	602 ± 124	11 (1.8%)	−79	100	1.00
	2.5–5 mm	352 ± 80	407 ± 120	61 (17.4%)	−28	150	0.29
	5–7.5 mm	193 ± 49	205 ± 60	15 (8.1%)	−36	66	1.00

* Mean values adjusted for age (64.1), sex (1.6), and BMI (28.7).

Table IV
Pair-wise comparison of tibial BMD measurements in patients with knee OA with 'no pain' and 'severe pain' while lying down at night, including mean ± SD, adjusted mean difference, percent difference from 'no pain', 95% confidence interval (CI), and *P*-value. Bolded values indicate $P < 0.05$

Region	Depth	BMD (mg/cm^3 K_2HPO_4)		Adjusted mean difference* from No Pain (%)	95% confidence interval (mg/cm^3 K_2HPO_4)		*P*-value
		No Pain	Severe Pain				
		Mean ± SD	Mean ± SD		Lower limit	Upper limit	
Medial plateau							
Total	0–2.5 mm	480 ± 93	406 ± 110	−76 (−15.8%)	−186	33	0.27
	2.5–5 mm	322 ± 98	251 ± 107	−74 (−22.7%)	−174	26	0.22
	5–7.5 mm	203 ± 85	154 ± 80	−54 (−25.8%)	−132	24	0.28
Focal BMD	0–2.5 mm	658 ± 94	595 ± 114	−66 (−9.9%)	−170	39	0.37
	2.5–5 mm	499 ± 130	399 ± 148	−102 (−20.3%)	−237	33	0.20
	5–7.5 mm	347 ± 135	258 ± 134	−90 (−25.7%)	−211	30	0.21
Lateral plateau							
Total	0–2.5 mm	339 ± 62	427 ± 74	85 (25.1%)	−6	176	0.07
	2.5–5 mm	198 ± 52	261 ± 61	62 (31.2%)	−10	133	0.11
	5–7.5 mm	127 ± 38	150 ± 38	22 (17.5%)	−22	66	0.64
Focal BMD	0–2.5 mm	596 ± 81	652 ± 54	58 (9.7%)	−47	163	0.53
	2.5–5 mm	352 ± 80	461 ± 71	114 (32.7%)	−10	218	**0.028**
	5–7.5 mm	193 ± 49	249 ± 55	60 (31.6%)	0	120	**0.049**

* Mean values adjusted for age (64.1), sex (1.6), and BMI (28.7).

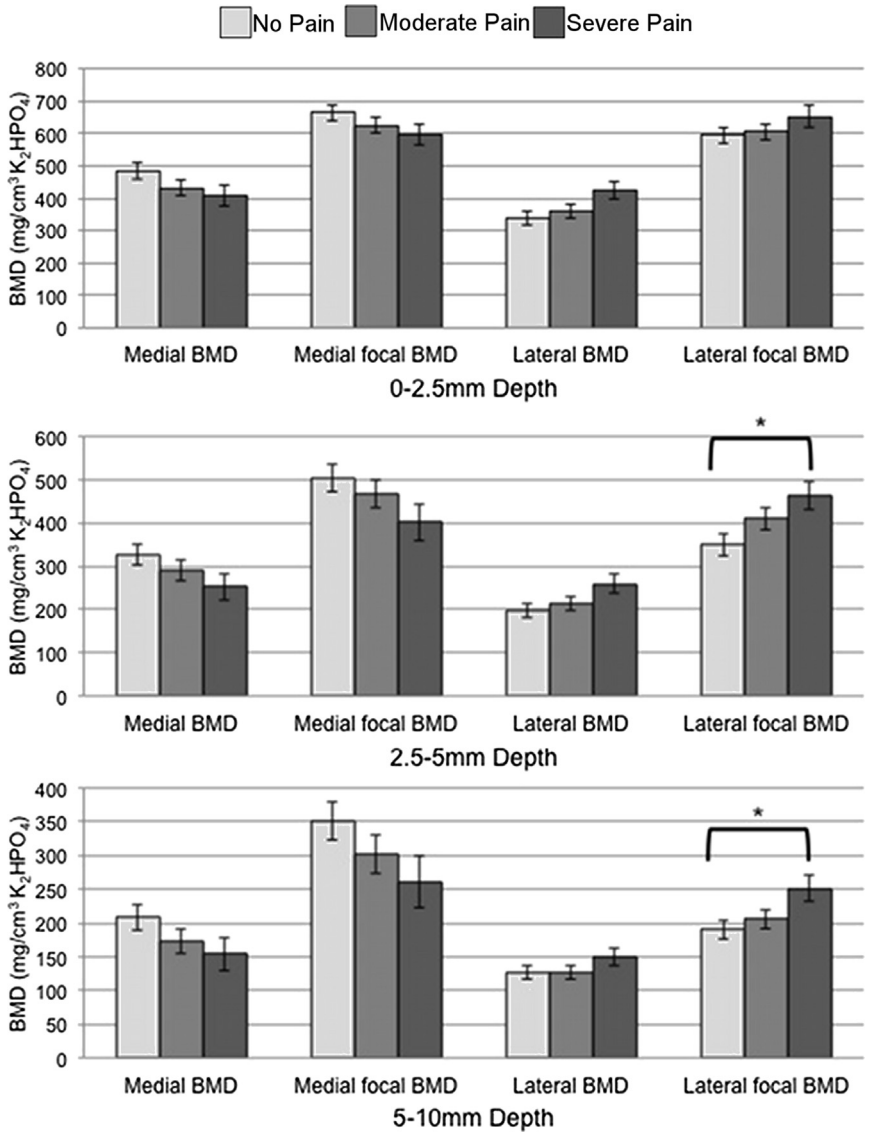

Fig. 2. Adjusted mean regional BMD of each group ('no pain', 'moderate pain', and 'severe pain') at depths of 0–2.5 mm, 2.5–5 mm, and 5–10 mm from the subchondral surface. Statistically significant differences ($P < 0.05$) between groups are noted with brackets. Error bars represent 95% confidence intervals.

BMD than surrounding bone tissue[11]. The logical ensuing assumption that higher BMD would be associated with pain is supported by our findings. Interestingly, higher BMD was found at depths greater than 2.5 mm from the subchondral surface in regions comprised primarily of trabecular bone, which parallels findings of BMLs predominantly in trabecular regions[16,17]. Given that trabecular bone is densely innervated[39], it is most likely an initiatory site for pain. Unfortunately, due to limited data, we are unsure if higher BMD measures coincide with BML presence. Further research is needed linking pain, BMD and BMLs using CT and MR co-registration techniques such as those employed by Lowitz *et al.*[11].

The results of this study give some insight into why the results from previous studies linking OA-related knee pain and proximal tibial subchondral bone density are conflicting. One study found an association between high aBMD and pain[20], where another found a relationship between low aBMD and pain[21]. The reasons for this disagreement may be due to inherent limitations of DXA. For example, patient size and positioning sensitivities may affect aBMD measurements whereby larger and mis-positioned patients have more bone in the projection direction, resulting in an overestimation of aBMD[22]. Also, there are no standardized ROI with DXA to evaluate proximal tibial subchondral aBMD, with ROIs varying in size and placement from study to study[12,21,23]. These ROIs most likely contain both subchondral cortical and trabecular bone. The results of this study suggest that sites distal to the subchondral surface (which contain primarily trabecular bone) appear to be most affected by OA. As such, aBMD measures containing both subchondral cortical and trabecular bone may not be sensitive enough to capture OA-effects on local bone density. Conversely, by evaluating BMD at specific depths from the subchondral surface, the depth-specific imaging technique used in this study was able to approximate individual effects of OA on regions composed of mostly mineralized subchondral cortical bone (0–2.5 mm layer) and trabecular bone (2.5–5 and 5–10 mm layers).

Another possible reason for disagreement between higher and lower aBMD and pain may be because previous studies reporting aBMD appear to have evaluated entire compartments of the proximal tibia[20,21]. This study found no associations between pain severity and BMD at the total lateral or medial plateau. Instead, our findings suggest that pain may be related to localized BMD differences[11], as indicated by the higher lateral focal 'spot' BMD in patients with 'severe pain' vs 'no pain' at depths of 2.5–5 mm and 5–10 mm from the subchondral surface. Further investigations, with depth-specific imaging techniques capable of measuring localized BMD, are needed to clarify the role of local subchondral bone density in OA-related pain.

Our results show higher BMD at the lateral plateau and a tendency for lower BMD at the medial plateau and as pain severity intensifies. These observations may be due to cyst presence and associated knee alignment. First, cyst presence may have been indirectly captured as low BMD measures, especially in the medial plateau. In this study, many of the individuals with 'severe pain' had CT evidence of cysts (moderate-to large-size and number), focused predominately in the medial plateau. Conversely, few individuals with 'no pain' had radiographic evidence of cysts of similar size and number. Interestingly, our BMD measures may be indirectly reflecting cyst size and number. Second, patients with 'severe pain' appear to have altered joint alignment and/or evidence of joint laxity with medial shifting of the femur relative to the tibia. Conversely, patients with 'no pain' had either varus or neutral alignment, with only one knee in valgus. This malalignment could result in loading-induced adaptation and lower medial BMD and higher lateral BMD[40]. This malalignment may be a consequence of advancing disease progression[41] or a consequence of self-adjusted joint alignment to help alleviate joint pain caused by other factors, such as medial cyst presence. Given that the lateral compartment has a smaller contact area then the medial compartment, and higher associated contact and interosseous stresses, it is possible that patients with valgus alignment are simply more susceptible to severe knee pain. It is possible that higher lateral BMD has influenced local innervation[18], leading to pain. Though, as noted earlier, observed higher lateral BMD may be a secondary effect caused by medial cyst presence.

Cyst findings generate an interesting hypothesis to explain why individuals with 'severe pain' had a trend for lower medial bone density than individuals with 'no pain'. Severe pain may be partly due to greater bone resorption and necrotic cyst development, both manifesting as low BMD. The 'bony contusion theory'[42,43] proposes that excessive loading or trauma causes trabecular microfractures, necrotic bone and focal bone resorption, eventually resulting in cyst development near the subchondral bone surface. Inflammatory macrophages within the lining of cysts are capable of forming into osteoclasts[44], which could promote further bone resorption and cyst expansion[45]. Bone surrounding cysts have been reported to be necrotic and lacking of blood vessels or normal marrow components[46], which could contribute to pain[47]. Local subchondral bone cyst presence is also thought to increase intra-osseous stress distributions, leading to pain and disability[48]. Given that cyst volumes range in size from 1 mm^3 to 657 mm^3 [49], which is much greater than QCT voxel volumes (0.244 mm^3 voxel volume; 0.625 × 0.625 × 0.625 mm voxel size), there is strong potential to develop novel QCT-based techniques for quantifying cyst volume and number to investigate this hypothesis further. However, multi-modality validation studies (e.g., microCT vs QCT) are first needed to verify that QCT-based techniques isolate cysts from surrounding subchondral bone and offer accurate measures of cyst size and number.

Strengths of this study include sample characteristics, the use of an internal control, normalization of our depth-specific measurements, and high degree of measurement precision. Our study sample was a homogeneous group of patients with similar OA severity and known covariates (age, sex, and BMI) between pain groups, possibly reducing the effect of possible confounding factors affecting BMD and pain. Also, we used tibial shaft cortical area and density measurements to account for possible between-group differences in systemic and/or local factors that may be associated with subchondral BMD. All BMD measurements were normalized according to mean proximal tibial volume and plateau surface area, and all imaged volumes were rotated and reoriented in similar 3D orientations relative to manually selected landmark boundary points and best-fit planes. This permitted reliable comparisons between groups. Lastly, we used a precise depth-specific image processing technique to assess plateau and focal BMD[33]. The observed differences in local BMD between 'severe pain' and 'no pain' groups were ~7× greater than associated precision errors[33], and are therefore trustworthy.

This study has certain limitations. First, pain severity and assessment was based on the entire knee joint, including all joint surfaces (tibiofemoral and patellofemoral) and tissues (e.g., bone, menisci, synovium), and it is uncertain if pain originated at the proximal tibial surface, other tissues, or a combination of surfaces and tissues. Second, although OA severity was homogeneous throughout study participants, all were in late stages of OA and it may not be possible to apply our findings to patients with less severe OA. Third, we used a bone reconstruction kernel (as opposed to a standard soft-tissue reconstruction kernel) to help distinguish the subchondral surface and ease segmentation. This reconstruction kernel may have overestimated BMD values very close to the subchondral surface. Fourth, our study sample size was small

($n = 42$), and with a basic rule of thumb of 10 samples per predictor[50], we were limited to four covariates (BMD, age, sex, BMI) and could not add additional covariates to our statistical analysis (e.g., cyst presence, knee alignment). Our small sample, combined with inherent measurement imprecision (albeit small), also likely explains why medial BMD, which appeared lower in the pain groups vs no pain group, did not reach statistical significance. Larger studies should be completed to confirm our findings and clarify the relationship between BMD and OA-related pain.

Depth-specific imaging techniques demonstrated higher lateral maximum focal BMD in patients with 'severe pain', compared to patients with 'no pain' at night in bed, at depths of 2.5–5 mm, and 5–10 mm from the proximal tibial subchondral surface. This study suggests that deep subchondral bone layers, as opposed to the bone immediately adjacent to the subchondral surface, may have a role in OA-related pain pathogenesis.

Author contributions

WDB carried out the image processing, participated in statistical analysis and interpretation of data, and composed the draft manuscript. SAK participated in statistical analysis and interpretation of data. CEM participated in study design and acquisition of patient data. DH participated in coordination of the study and acquisition of patient data. CT participated in study design, participant recruitment and acquisition of patient data. DJH participated in study design and coordination of the study. DRW participated in study design. JDJ conceived the study, assisted in image processing, and interpretation of data. All authors revised and/or critically evaluated the draft manuscript. All authors read and approved the final manuscript.

Conflict of interest

Nothing to declare. The corresponding author had full access to all the data in the study and had final responsibility for the decision to submit for publication.

Acknowledgements

This project was funded through support from the Canadian Arthritis Network (CAN) (Grant 09-02-PGP-02) and New England Baptist Hospital Research Funding Awards.

References

1. Cooper C, McAlindon T, Coggon D, Egger P, Dieppe PA. Occupational activity and osteoarthritis of the knee. Ann Rheum Dis 1994;53:90–3.
2. Hunter DJ, Felson DT. Osteoarthritis. Br Med J 2006;332(7542):639–42.
3. Hawker GA, Stewart L, French MR, Cibere J, Jordan JM, March L, *et al*. Understanding the pain experience in hip and knee osteoarthritis – an OARSI/OMERACT initiative. Osteoarthritis Cartilage 2008;16:415–22.
4. Lo GH, McAlindon TE, Niu J, Zhang Y, Beals C, Dabrowski C, *et al*. Bone marrow lesions and joint effusion are strongly and independently associated with weight-bearing pain in knee osteoarthritis: data from the osteoarthritis initiative. Osteoarthritis Cartilage 2009;17(12):1562–9.
5. Dieppe P, Lohmander L. Pathogenesis and management of pain in osteoarthritis. Lancet 2005;365(9463):965–73.
6. Woolhead G, Gooberman-Hill R, Dieppe P, Hawker G. Night pain in hip and knee osteoarthritis: a focus group study. Arthritis Care Res 2010;62(7):944–9.
7. Buckland-Wright C. Subchondral bone changes in hand and knee osteoarthritis detected by radiography. Osteoarthritis Cartilage 2004;12:10.
8. Bobinac D, Spanjol J, Zoricic S, Maric I. Changes in articular cartilage and subchondral bone histomorphometry in osteoarthritic knee joints in humans. Bone 2003;32(3):284–90.
9. Zysset PK, Sonny M, Hayes WC. Morphology-mechanical property relations in trabecular bone of the osteoarthritic proximal tibia. J Arthroplasty 1994;9(2):203–16.
10. Johnston JD, Kontulainen SA, Masri BA, Wilson DR. A comparison of conventional maximum intensity projection with a new depth-specific topographic mapping technique in the CT analysis of proximal tibial subchondral bone density. Skeletal Radiol 2010;39(9):867–76.
11. Lowitz T, Museyko O, Bousson V, Laouisset L, Kalendar WA, Laredo JD, *et al*. Bone marrow lesions identified by MRI in knee osteoarthritis are associated with locally increased bone mineral density measured by QCT. Osteoarthritis Cartilage 2013;21(7):957–64.
12. Lo GH, Hunter DJ, Zhang Y, McLennan CE, LaValley MP, Kiel DP, *et al*. Bone marrow lesions in the knee are associated with increased local bone density. Arthritis Rheum 2005;52(9):2814–21.
13. Yusuf E, Kortekaas MC, Watt I, Huizinga TWJ, Kloppenburg M. Do knee abnormalities visualised on MRI explain knee pain in knee osteoarthritis? A systematic review. Ann Rheum Dis 2011;70(1):60–7.
14. Felson DT, Niu J, Guermazi A, Roemer FW, Aliabadi P, Clancy M, *et al*. Correlation of the development of knee pain with enlarging bone marrow lesions on magnetic resonance imaging. Arthritis Rheum 2007;56(9):2986–92.
15. Driban JB, Price LL, Lo GH, Pang J, Hunter DJ, Miller E, *et al*. Evaluation of bone marrow lesion volume as a knee osteoarthritis biomarker – longitudinal relationships with pain and structural changes: data from the Osteoarthritis Initiative. Arthritis Res Ther 2013;15(5):R112.
16. Sowers M. Magnetic resonance-detected subchondral bone marrow and cartilage defect characteristics associated with pain and X-ray-defined knee osteoarthritis. Osteoarthritis Cartilage 2003;11(6):387–93.
17. Torres L, Dunlop D, Peterfy C, Guermazi A, Prasad P, Hayes K, *et al*. The relationship between specific tissue lesions and pain severity in persons with knee osteoarthritis. Osteoarthritis Cartilage 2006;14(10):1033–40.
18. Mach DB, Rogers SD, Sabino MC, Luger NM, Schwei MJ, Pomonis JD, *et al*. Origins of skeletal pain: sensory and sympathetic innervation of the mouse femur. Neuroscience 2002;113(1):155–66.
19. Radin EL, Paul IL, Rose RM. Role of mechanical factors in pathogenesis of primary osteoarthritis. Lancet 1972;1(7749):519–22.
20. Akamatsu Y, Mitsugi N, Taki N, Ashi HK, Saito T. Medial versus lateral condoyle bone mineral density ratios in a cross-sectional study: a potential marker for medial knee osteoarthritis severity. Arthritis Care Res 2012;64(7):1036–45.
21. Dore D, Ding C, Jones G. A pilot study of the reproducibility and validity of measuring knee subchondral bone density in the tibia. Osteoarthritis Cartilage 2008;16(12):1539–44.
22. Watts NB. Fundamentals and pitfalls of bone densitometry using dual-energy X-ray absorptiometry (DXA). Osteoporos Int 2004;15(11):847–54.
23. Beattie KA, Boulos P, Duryea J, O'Neill J, Pui M, Gordon CL, *et al*. The relationships between bone mineral density in the spine, hip, distal femur and proximal tibia and medial minimum joint

space width in the knees of healthy females. Osteoarthritis Cartilage 2005;13(10):872–8.
24. Johnston JD, Masri BA, Wilson DR. Computed tomography topographic mapping of subchondral density (CT-TOMASD) in osteoarthritic and normal knees: methodological development and preliminary findings. Osteoarthritis Cartilage 2009;17(10):1319–26.
25. Burnett WD, Kontulainen SA, McLennan CE, Wilson DR, Hunter DJ, Johnston JD. Regional depth-specific subchondral bone density measures in osteoarthritic and normal patellae: in vivo precision and preliminary comparisons. Osteoporos Int 2014;25(3):1107–14.
26. Kellgren JH, Lawrence JS. Radiological assessment of osteo-arthrosis. Ann Rheum Dis 1957;16:494–502.
27. Bellamy N, Buchanan WW, Goldsmith CH, Campbell J, Stitt LW. Validation study of WOMAC: a health status instrument for measuring clinically important patient relevant outcomes to antirheumatic drug therapy in patients with osteoarthritis of the hip or knee. J Rheumatol 1988;15(12):1833–40.
28. Altman RD, Gold GE. Atlas of individual radiographic features in osteoarthritis, revised. Osteoarthritis Cartilage 2007;15(Suppl A):A1–A56.
29. Drum MG, Les CM, Park RD, Norrdin RW, McIlwraith CW, Kawcak CE. Correlation of quantitative computed tomographic subchondral bone density and ash density in horses. Bone 2009;44(2):316–9.
30. Schneider S, Breit SM, Grampp S, Kunzel WW, Liesegang A, Mayrhofer E, *et al*. Comparative assessment of bone mineral measurements obtained by use of dual-energy x-ray absorptiometry, peripheral quantitative computed tomography, and chemical-physical analyses in femurs of juvenile and adult dogs. Am J Vet Res 2004;65(7):891–900.
31. Kontulainen SA, Johnston JD, Liu D, Leung C, Oxland TR, McKay HA. Strength indices from pQCT imaging predict up to 85% of variance in bone failure properties at tibial epiphysis and diaphysis. J Musculoskelet Neuronal Interact 2008;8(4):401–9.
32. Davidson PL, Mahar B, Chalmers DJ, Wilson BD. Impact modeling of gymnastic back-handsprings and dive-rolls in children. J Appl Biomech 2005;21(2):115–28.
33. Johnston JD, McLennan CE, Hunter DJ, Wilson DR. In vivo precision of a depth-specific topographic mapping technique in the CT analysis of osteoarthritic and normal proximal tibial subchondral bone density. Skeletal Radiol 2010;40(8):1057–64.
34. Gluer CC, Blake G, Lu Y, Blunt BA, Jergas M, Genant HK. Accurate assessment of precision errors: how to measure the reproducibility of bone densitometry techniques. Osteoporos Int 1995;5(4):262–70.
35. Spoor CF, Zonneveld FW, Macho GA. Linear measurements of cortical bone and dental enamel by computed tomography: applications and Problems. Am J Phys Anthropol 1993;91:469–84.
36. Yamada K, Healey R, Amiel D, Lotz M, Coutts R. Subchondral bone of the human knee joint in aging and osteoarthritis. Osteoarthritis Cartilage 2002;10(5):360–9.
37. Frank AW, Labas MC, Johnston JD, Kontulainen SA. Site-specific variance in radius and tibia bone strength as determined by muscel size and body mass. Physiother Can 2012;64(3):292–301.
38. Seah S, Wheaton D, Li L, Dyke JP, Talmo C, Harvey WF, *et al*. The relationship of tibial bone perfusion in knee osteoarthritis. Osteoarthritis Cartilage 2012;20:1527–33.
39. Chen B, G-x Pei, Jin D, K-h Wei, Qin Y, Qing-si L. Distribution and property of nerve fibers in human long bone tissue. Chin J Traumatol 2007;10(1):3–9.
40. Wada M, Maezawa Y, Baba H, Shimada S, Sasaki S, Nose Y. Relationships among bone mineral densities, static alignment and dynamic load in patients with medial compartment knee osteoarthritis. Rheumatology (Oxford) 2001;40(5):499–505.
41. Hunter DJ, Sharma L, Skaife T. Alignment and osteoarthritis of the knee. J Bone Joint Surg 2009;91(Suppl 1):85–9.
42. Durr HD, Martin H, Pellengahr C, Schlemmer M, Maier M, Jansson V. The cause of subchondral bone cysts in osteo-arthrosis: a finite element analysis. Acta Orthop Scand 2004;75(5):554–8.
43. Ondrouch AS. Cyst formation in osteoarthritis. J Bone Joint Surg Br 1963;45:755–60.
44. Sabokbar A, Crawford R, Murray DW, Athanasou NA. Macrophage-osteoclast differentiation and bone resorption in osteo-arthrotic subchondral acetabular cysts. Acta Orthop Scand 2000;71(3):255–61.
45. von Rechenberg B, Leutenegger C, Zlinsky K, McIlwraith CW, Akens MK, Auer JA. Upregulation of mRNA of interleukin-1 and -6 in subchondral cystic lesions of four horses. Equine Vet J 2001;33(2):143–9.
46. McErlain DD, Ulici V, Darling M, Gati JS, Pitelka V, Beier F, *et al*. An in vivo investigation of the initiation and progression of subchondral cysts in a rodent model of secondary osteoarthritis. Arthritis Res Ther 2012;14(1):R26.
47. Fondi C, Franchi A. Definition of bone necrosis by the pathologist. Clin Cases Miner Bone Metab 2007;4(1):21–6.
48. McErlain DD, Milner JS, Ivanov TG, Jencikova-Celerin L, Pollmann SI, Holdsworth DW. Subchondral cysts create increased intra-osseous stress in early knee OA: a finite element analysis using simulated lesions. Bone 2011;48(3):639–46.
49. Chiba K, Burghardt AJ, Osaki M, Majumdar S. Three-dimensional analysis of subchondral cysts in hip osteoarthritis: an ex vivo HR-pQCT study. Bone 2014;66:140–5.
50. Peduzzi P, Concato J, Kemper E, Holford TR, Feinstein AR. A simulation study of the number of events per variable in logistic regression analysis. J Clin Epidemiol 1996;49(12):1373–9.